IOP Publishing | Astro Ltd
Laser Physics Letters
Laser Phys. Lett. **14** (2017) 015601 (8pp)
doi:10.1088/1612-202X/aa4fc1

Letter

Diffuse optical spectroscopy monitoring of oxygen state and hemoglobin concentration during SKBR-3 tumor model growth

A G Orlova[1,2], M Yu Kirillin[1], A B Volovetsky[2], N Yu Shilyagina[2], E A Sergeeva[1], G Yu Golubiatnikov[1] and I V Turchin[1]

[1] Institute of Applied Physics, Russian Academy of Sciences, 46 Ulyanov Street, Nizhny Novgorod 603950, Russia
[2] N.I. Lobachevsky State University of Nizhny Novgorod, 603000 Gagarin Avenue, 23, Nizhny Novgorod, Russia

E-mail: orlova@ufp.appl.sci-nnov.ru

Received 11 November 2016
Accepted for publication 21 November 2016
Published 7 December 2016

Abstract

Tumor oxygenation and hemoglobin content are the key indicators of the tumor status which can be efficiently employed for prognosis of tumor development and choice of treatment strategy. We report on monitoring of these parameters in SKBR-3 (human breast adenocarcinoma) tumors established as subcutaneous tumor xenografts in athymic nude mice by diffuse optical spectroscopy (DOS). A simple continuous wave fiber probe DOS system is employed. Optical properties extraction approach is based on diffusion approximation. Statistically significant difference between measured values of normal tissue and tumor are demonstrated. Hemoglobin content in tumor increases from 7.0 ± 4.2 μM to 30.1 ± 16.1 μM with tumor growth from $150 \pm 80\,\mathrm{mm}^3$ to $1300 \pm 650\,\mathrm{mm}^3$ which is determined by gradual increase of deoxyhemoglobin content while measured oxyhemoglobin content does not demonstrate any statistically significant variations. Oxygenation in tumor falls quickly from $52.8 \pm 24.7\%$ to $20.2 \pm 4.8\%$ preceding acceleration of tumor growth. Statistical analysis indicated dependence of oxy-, deoxy- and total hemoglobin on tumor volume ($p < 0.01$). DOS measurements of oxygen saturation are in agreement with independent measurements of oxygen partial pressure by polarography (Pearson's correlation coefficient equals 0.8).

Keywords: diffuse optical spectroscopy, oxygen saturation, hemoglobin, tumor model

(Some figures may appear in colour only in the online journal)

1. Introduction

Malignant tumor is a complex biological system consisting of cancer cells surrounded by various cellular and non-cellular components forming tumor microenvironment [1]. Tumor development parameters, such as tumor growth, invasion and metastasis formation are determined by the characteristics of the tumor microenvironment, in particular, tumor blood flow parameters, such as angiogenesis, perfusion, microcirculation, vascular permeability and oxygenation level [2, 3]. Abnormal vascular structure is a typical feature of many solid tumors: tumors vascular network is immature, primitive and chaotic comparing to normal tissues. Vascular alterations in tumors lead to slowing down blood flow and, consequently, oxygen supply deterioration. As a result of an imbalance between tissue oxygen delivery and consumption, oxygen partial pressure (pO_2) value reduces arising hypoxia. Hypoxic tumor becomes resistant to the action of a therapeutic agent, and also

stimulates a number of genes that are responsible for activation of tumor growth, metastasis and angiogenesis [4–6]. In this respect, diagnostics of hypoxia and revealing its origin remain ones of the most essential problems in experimental and clinical oncology and cost-effective techniques for *in vivo* monitoring of tissue oxygen status are still required.

Optical properties of blood-containing biotissues are known to significantly depend on blood oxygenation due to significant difference in absorption spectra of oxy- and deoxyhemoglobin. Spectroscopic measurements data enable reconstructing concentration of tissue principal chromophores: oxy- (HbO_2), deoxyhemoglobin (HHb), water and lipids by their absorption [7]. This information allows for indirect evaluation of the oxygen state of biological tissues and concluding on the main mechanisms of oxygenation changes. Total hemoglobin concentration ($[tHb] = [HHb] + [HbO_2]$) is an indicator of blood content, while alterations in oxygen consumption rate and oxygen supply can be indirectly reflected by changes of deoxyhemoglobin and oxyhemoglobin concentrations, respectively. Effect of blood inflow and outflow rates on concentrations of oxygenated and deoxygenated forms of hemoglobin (Hb) also should be taken into account [8].

Currently, a number of methods for non-invasive *in vivo* determination of particular morphological and functional parameters of tumor vascular bed are developed and successfully used in experimental and clinical oncology [9, 10]. Diffuse optical spectroscopy (DOS) technique allows for simultaneous assessment of several parameters characterizing the mechanisms underlying changes in neoplasm oxygenation level. The DOS is based on reconstruction of optical properties of biological tissues (absorption and scattering coefficients) basing on spectral detection of probing radiation scattered from tissues under study [7]. DOS measurements are usually performed in transmittance or reflectance modes depending on mutual location of sources and detectors with respect to the object under study. However, due to strong attenuation in biotissues reflectance mode is preferable as it does not require employment of extremely sensitive photodetectors when the object optical thickness is quite large. Besides, in reflectance mode the measurement volume can be controlled more accurately by choice of proper source-detector separation distance.

Current promising DOS applications include cancer diagnostics in clinical oncology [11–13] and studies of tumor hypoxia formation and analysis of mechanisms of therapeutic action on preclinical tumor models in experimental oncology [14–17].

Diffuse reflectance spectroscopy study revealed the decrease of tumor oxygenation during its natural growth in mouse breast carcinoma model was reported in [14]. However, the same group demonstrated increase in blood oxygen saturation level in murine head and neck xenografts [15]. A rapid decrease of oxygenation of mammary tumors in course of their growth in mice was also shown [16]. Thus, one can conclude that the data derived from DOS measurements on the dynamics of experimental tumor oxygenation during tumor growth is contradictory. Trends in tumor oxygenation dynamics vary significantly and may depend on the tumor model type. In this respect, further studies of the oxygenation dynamics during natural tumor growth are of importance.

In this study, we monitor the dynamics of oxygen saturation in tumors during its growth together with oxygen saturation in normal tissue. We used reflectance configuration of diffuse optical spectroscopy to *in vivo* determine the oxygenation level in animal model of human breast cancer SKBR-3 and to reveal its evolution mechanisms in the course of tumor growth. Visible spectral range (530–650 nm) was used for analysis similar to other studies [11, 18, 19], as oxy- and deoxyhemoglobin exhibit maximal differences in this range while light penetration depth is sufficient for probing superficial tissues. Differences in oxygenation and blood content of experimental tumors and normal tissues have been demonstrated. Gradual increase in blood content accompanied by decrease of oxygenation level has been also shown during tumor growth. Simultaneously, the increase in the content of deoxyhemoglobin occurs, characterizing such processes as the tissue oxygen consumption rise and/or blood outflow fall. Due to the fact that the decrease in the oxygenation level accompanied by increasing blood filling, it is possible to assume a greater contribution of disorder in blood outflow from the tumor with increasing tumor nodule size. Strong positive correlation between the tumor volume and hemoglobin content has been demonstrated. Data on blood oxygen saturation StO_2 obtained by the optical method for the normal and tumor tissue were confirmed by the data of polarographic measurement of oxygen partial pressure pO_2.

2. Materials and methods

2.1. Tumor model and animal study design

The experiments were carried out on Balb/c-nude female athymic mice 16–20 g (6 animals). The animals were obtained from the Nursery for laboratory animals 'Pushchino' (Moscow, Russia). For development of the xenograft model of human breast cancer cell line SKBR-3 (human breast adenocarcinoma, ATCC number HTB-30) was used. Cells were cultured in McCoy's 5A medium (HyClone, USA). The growth medium contained 10% fetal calf serum (HyClone, USA) and 2 mM L-glutamine (PanEco, Russia). Cultivation was performed at 37 °C in an atmosphere with 5% CO_2. At each stage of passaging cells treated with a Versene Solution (PanEco, Russia). The suspension of cells (5 million) in 10 mM phosphate-buffered saline PBS (100 μl) was inoculated subcutaneously into the outer side of the left thigh. Experiments were carried out in accordance with international rules of legal and ethical use of animals.

The DOS measurements were performed daily for 11 d starting from the 12th day after tumor inoculation, when the tumors reached 5–10 mm in diameter to ensure that all collected probing radiation comes from the tumor. Tumor size was measured daily by the caliper in three mutually perpendicular directions and the tumor volume was calculated by the following formula:

$$v = \frac{abc}{2}, \tag{1}$$

where a, b, and c are the measured tumor linear dimensions.

Diffuse optical spectra were measured from the animal body surface in the tumor region and in the normal muscle region (right thigh). For verification of DOS data, pO_2 was measured in the tissues by polarographic method at 12th, 16th, 19th, and 22nd days of tumor growth in two mice in the tumor and muscle tissues. To measure pO_2 in the tissues Clark microelectrode OX-N (Unisense, Denmark) and picoamperemeter V7-49 (Russia) were used.

Tumor size measurements and DOS measurements were performed on unanesthetized animals. For polarography, before the introduction of the probing needle of OX-N microelectrode into the animal tissue, mice were anesthetized by intraperitoneal injection of a mixture of Zoletil 100 (Virbac, France) in the concentration of 20 mg ml^{-1} (50 μl per animal) with 10 μl of 2% Rometar (Bioveta, Czech Republic).

2.2. Diffuse optical spectroscopy system

The DOS system based on the one previously described in details in [20] is used in the experiment. The system uses Tungusten halogen lamp LS-1-LL (Ocean Optics Inc., USA) (spectral range: 400–900 nm; output power of 6.5 mW) as a probing light source. Probing radiation is delivered to the tissue surface through a 200 μm optical fiber (Polironic Ltd, Russia). Scattered radiation is collected from the surface by detecting fiber located at 1.5 mm from the probing one. Collected radiation is registered by S2000 spectrometer (Ocean Optics, Inc. USA). The source-detector separation distance is 1.5 mm to ensure large enough signal at the detector yielding the estimated probing depth of about half of this distance [7]. Thus, the measurement volume included skin (reaching up to 400 μm in thickness [21]) and underlying tumor/muscle tissue. Blood content for skin of mice was estimated to be lower or similar to skeletal muscle [22], however, due to the banana shape of the measurement volume the contribution of the superficial skin layer to extracted absorption coefficient value is lower compared to that from the underlying tissue.

2.3. Extraction of tissue physiological properties from the measured spectra

The algorithm for extraction of the exact values of concentrations of tHb, HHb, HbO_2, and StO_2 consists of two steps: at the first step the absorption coefficient spectra are derived from DOS measurements using the algorithm based on diffusion theory; at the second step concentrations of HHb and HbO_2 are reconstructed.

When reconstructing absorption coefficient spectra we assume that the registered intensity at the detector can be described in the frames of diffusion theory as:

$$I(\lambda, r) = \frac{CI_0(\lambda)\mu_t'}{r} e^{-\sqrt{3\mu_a\mu_t'}r} \quad (2)$$

where $I_0(\lambda)$ is the probing radiation intensity spectrum, C is the dimensionless constant depending on source and detector parameters (fiber apertures, fiber-tissue interfaces, detector quantum yield and amplification, etc), r is source-detector separation, μ_a and $\mu_t' = \mu_s(1-g) + \mu_a$ are absorption and transport coefficients, respectively; μ_s is scattering coefficient and g is anisotropy factor. Probing radiation spectrum $I_0(\lambda)$ was measured before each measurement to account for possible alterations of the source power. The value of the constant C was derived from the model experiment with Lipofundin and ink based tissue optical phantom with known optical properties [23]. Optical properties of the phantom were measured by spectrophotometry technique with Analytikjena Specord 250PLUS spectrophotometer equipped with an integrating sphere. For simplification of the reconstruction we assumed that scattering in tissue significantly exceeds absorption and, hence, variations of μ_t' can be neglected. Absorption spectrum was calculated from formula (2). Values for μ_t' employed in the reconstruction were measured earlier by spectrophotometry technique for murine muscle *ex vivo* [23].

At the second stage of reconstruction it is assumed that in the spectral range of 500–650 nm HHb, HbO_2 and water are the main tissues choromophores. In this connection the derived absorption coefficient spectrum was treated as the linear combination of absorption spectra of these three chromophores. Absorption spectra for HHb, HbO_2, and water are obtained from [24]. Non-negative least squares approach was employed to determine corresponding coefficients allowing to calculate tissue parameters, such as oxygen saturation, and hemoglobin content. Reconstruction algorithm was approbated in a model experiment with blood-containing Lipofundin-based tissue phantom.

2.4. Statistical analysis

All statistical calculations were performed with Statistica 6.0 (StatSoft), Matlab and Microsoft Excel software. Tumor volume values and extracted values of tHb, HbO_2, HHb concentrations as well as StO_2 levels are presented as means and standard deviations. The t-test for dependent samples was performed to determine the statistical significance difference between the values of these parameters at different time points from the baseline. The t-test for independent samples was employed for values obtained from tumor and muscle tissues. P values below 0.05 were considered to be statistically significant. Pearson's correlation coefficient (r) was calculated in order to establish correlation between the StO_2 values and pO_2 values (tumor and muscle together). Statistical hypothesis of independence between parameters of tumor volume and HHb, tumor volume and HbO_2, tumor volume and StO_2, tumor volume and tHb were tested using χ^2-test. The range of values of each parameter was divided into three equal segments. Further, based on the boundaries of these segments the characteristic values were grouped and 3×3 contingency tables were constructed. The hypothesis of independence was rejected if the p-value less than 0.05.

3. Results

Figure 1 shows the dynamics of SKBR-3 tumor growth starting from the 12th day after tumor inoculation (beginning of monitoring period). During the monitoring period the tumor

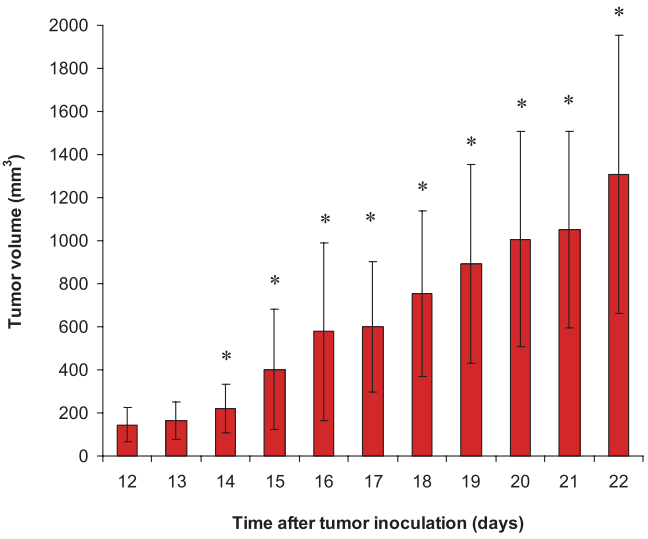

Figure 1. Dynamics of SKBR-3 volume during tumor growth. Asterisk (*) indicates statistically significant differences with the initial level at the beginning of monitoring period ($p < 0.05$).

volume increased up to 9 times from $150 \pm 80\,\mathrm{mm}^3$ to $1300 \pm 650\,\mathrm{mm}^3$ on the 22nd day after inoculation ($p < 0.01$). Statistically significant volume changes compared to baseline ($p = 0.03$) occurred on the day 14 after tumor cells injection. Dynamics of tumor growth of SKBR-3 is in accordance with the data reported in [25] for the same tumor model.

Figure 2 shows typical measured spectra and reconstructed absorption coefficient spectra of tumor and muscle tissues of Balb/c-nude mouse, obtained by DOS on the days 12, 16, 19, 22 after tumor inoculation. In the beginning of the monitoring period the tumor absorption coefficient spectrum shape is similar to that obtained for muscle tissue (figures 2(c) and (d), day 12). This implies similar content of chromophores in tumor and in normal tissue at this stage of tumor development. During the monitoring period the spectrum for muscle tissue demonstrates only insignificant variations (figure 1(d)). At the same time as the tumor grow absorption in the typical hemoglobin absorption band increases significantly (figure 2(c)) indicating increase in hemoglobin concentration and, hence, increase in blood content.

Calculation of the blood oxygen saturation level (figure 3) from the DOS spectral data (figure 2) shows that on day 12 of tumor growth the values in the tumor ($52.8 \pm 24.7\%$) do not differ significantly ($p = 0.43$) from those in the muscle tissue ($68.7 \pm 19.5\%$). However, starting from day 14 of tumor growth decreased StO_2 level in tumor tissue is observed. The differences are manifested as compared to baseline ($p = 0.04$) and to normal muscle tissue ($p < 0.01$). The level of blood oxygen saturation remained reduced for approximately three times starting from 14th up to 22nd day after tumor inoculation when it reached $20.2 \pm 4.8\%$. The observed reduced StO_2 level indicates reduced oxygenation in the tumor tissue in this time interval. It should be noted that a reduction of oxygen saturation to a constant level is fast enough and occurred from 12th to 14th day of tumor development.

The pO_2 values obtained by polarography in SKBR-3 starting from the day 16 of tumor development ranges from 3 to 30 mm Hg (figure 4). In general, the pO_2 values of the SKBR-3 indicate this tumor as a hypoxic one which is in agreements with the low blood oxygen saturation values derived from DOS measurements, the pO_2 values obtained for muscle vary between 20 and 70 mm Hg which also agrees with higher blood oxygenation level in muscle obtained by DOS as compared to tumor. Pearson correlation coefficient for the values of StO_2 and pO_2 obtained for the tumor and muscle is 0.8 ($p < 0.05$).

Average total hemoglobin concentration in tumor at the initial day of monitoring (12 d after tumor injection) was similar to that in muscle tissue (figure 5) amounting 7.0 ± 4.2 μM and 5.5 ± 3.8 μM, respectively. Differences in content of tHb with the baseline ($p < 0.01$) as well as between the tumor and muscle were detected on day 15 of tumor growth ($p = 0.03$). Further, total hemoglobin concentration continued to increase gradually reaching 30.1 ± 16.1 μM on day 22. The latter may indicate a gradual increase in blood content of SKBR-3 tumor in the period between 12th–22nd days of its natural growth.

No statistically significant alterations of tumor and muscle oxyhemoglobin concentrations and differences between them were revealed during the monitoring period (figure 6). HbO_2 values in tumor and in muscle amounted 4.1 ± 2.3 μM and 3.3 ± 1.3 μM ($p = 0.45$), respectively, on the 12th day and 7.2 ± 4.0 μM and 9.0 ± 2.9 μM ($p = 0.39$), respectively, on the 22nd day of tumor development. This may indicate the absence of significant changes in delivery of oxygen to tumor tissue during the monitoring period.

A gradual increase in concentration of deoxyhemoglobin was observed in the course of tumor growth (figure 7). On the 12th day of tumor development it was close to that of normal muscle tissue (4.0 ± 2.5 μM and 2.9 ± 2.8 μM, respectively). Changes in SKBR-3 HHb concentration became statistically significant comparing to the muscle ($p < 0.01$) and to the baseline starting from the 15th day of tumor growth ($p < 0.01$). By the end of the experiment (22nd day of tumor development) the value of deoxyhemoglobin concentration in tumor reached 27.9 ± 8.5, which is 7 times higher than that in muscle at the same day. This may be an indicator of significant changes in tumor oxygen consumption and/or tumor blood outflow during its natural growth.

Dependence of StO_2, tHb, HbO_2, and HHb on tumor node volume is analyzed. We demonstrate that rise in the level of different hemoglobin forms is associated with an increase in tumor node size. Strong dependence of the tHb, HbO_2, and HHb concentrations on tumor node volume (with significance level $p < 0.01$) is revealed (figures 8(a), (c) and (d)), while the values of StO_2 and tumor volume (figure 8(b)) were shown to be independent ($p = 0.11$).

4. Discussion

The main causes of tumor hypoxia are such cell properties as high metabolic activity and proliferation rate determining increased oxygen consumption in a neoplasm and vascular abnormalities determining decreased oxygen delivery [26].

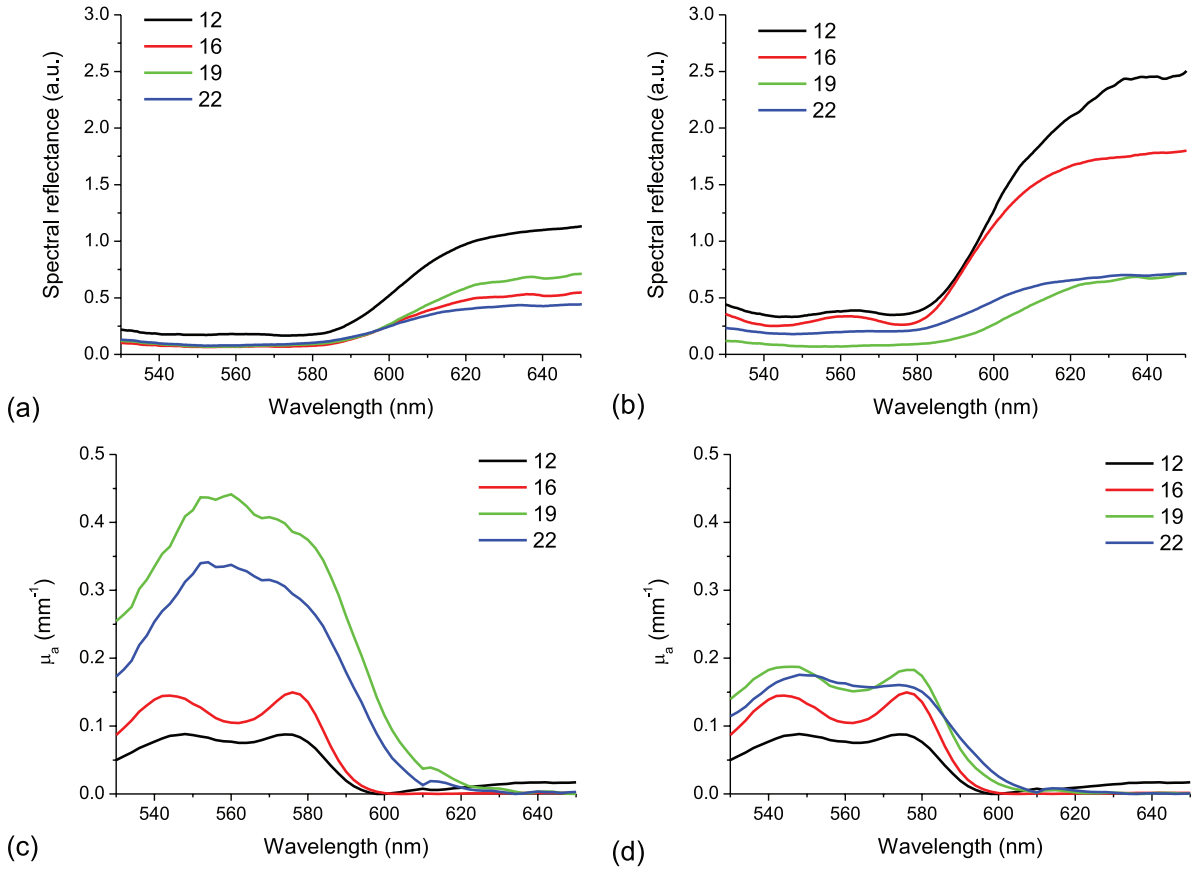

Figure 2. Typical normalized reflectance spectra (a) and (b) and reconstructed spectra of absorption coefficient (c) and (d) for tumor (a) and (c) and muscle (b) and (d) tissue at days 12, 16, 19, and 22 of tumor growth.

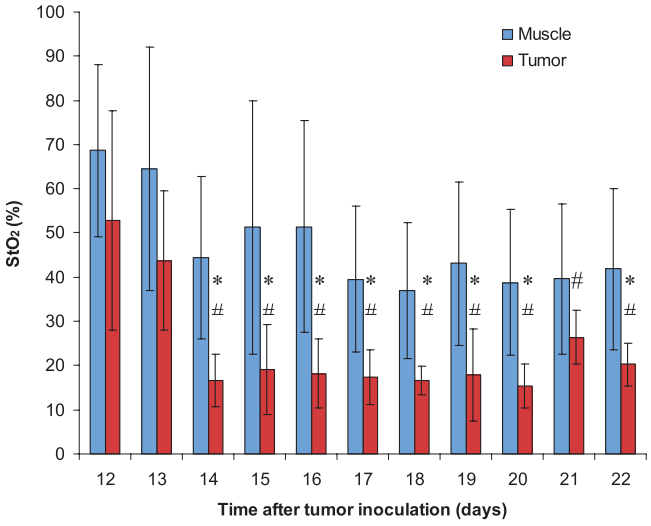

Figure 3. Dynamics of blood oxygen saturation level in SKBR-3 tumor and muscle. Asterisk (*) indicates statistically significant difference between the current and the initial values for tumor ($p < 0.05$). Hash (#) indicates statistically significant difference between current values for tumor and muscle ($p < 0.05$).

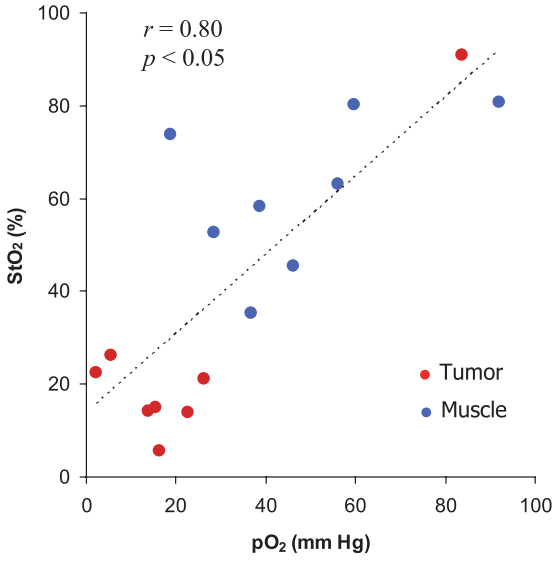

Figure 4. Oxygen saturation (StO_2) versus pO_2 values in tumor and in muscle (measurements from 12th, 16th, 19th, and 22nd days of tumor growth, r is the Pearson's correlation coefficient).

Development of novel approaches to study of the mechanisms of hypoxia formation is essential for a better understanding of its biological nature and for development of the methods for oxygen state correction.

We used DOS technique to study the dynamics of experimental SKBR-3 tumor oxygenation and blood content in the course of its natural growth. During monitoring SKBR-3 tumor we revealed the increase of hemoglobin concentration (figure 5) which indicates increased blood content, and decrease in blood oxygen saturation level (figure 3) which characterizes decreased oxygenation. Difference between the values of tHb and StO_2 in tumor and in normal tissue of experimental animals appears on day 14 after tumor inoculation.

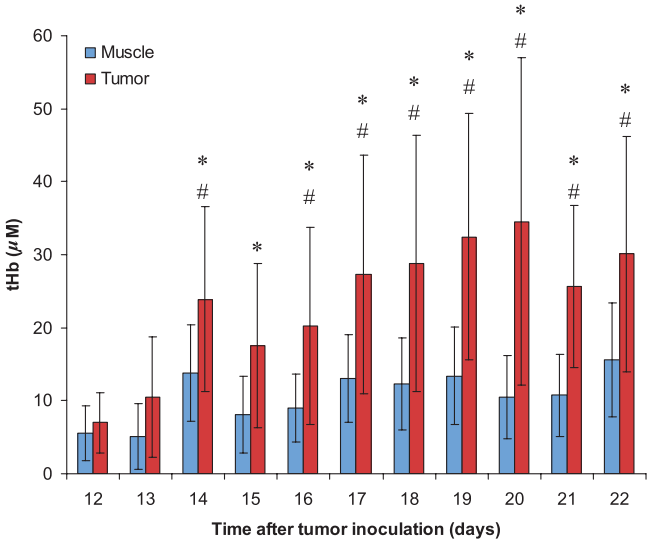

Figure 5. Dynamics of total hemoglobin concentration in tumor and muscle. Asterisk (*) indicates statistically significant difference between the current and the initial values for tumor ($p < 0.05$). Hash (#) indicates statistically significant difference between current values for tumor and muscle ($p < 0.05$).

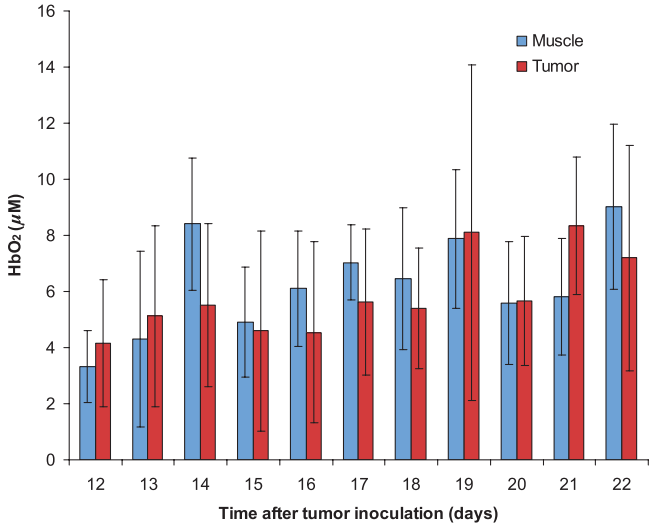

Figure 6. Dynamics of oxyhemoglobin concentration in SKBR-3 tumor and in muscle. Asterisk (*) indicates statistically significant difference between the current and the initial values for tumor ($p < 0.05$). Hash (#) indicates statistically significant difference between current values for tumor and muscle ($p < 0.05$).

The gradual growth of SKBR-3 tumor blood content was observed in parallel with an increase of tumor volume. Unlike the changes of blood content, reduction of tumor oxygenation level occurred quickly and preceded acceleration of tumor growth. Probably, this early change underlies the absence of dependence between the values of StO_2 and tumor volume. Simultaneous DOS assessment of oxygenated and deoxygenated forms of hemoglobin allows to conclude on the reasons of blood content and oxygenation variations. We demonstrate that for SKBR-3 the main contribution to the change of the blood content and oxygenation originates from deoxyhemoglobin accumulation (figure 7). This can be associated either with the increase of tissue oxygen consumption or/and with the decreased blood outflow. Insufficient level of oxygen supply, tumor expansion away from the vessel wall, and high oxygen demand of actively proliferating tumor may become the reasons of high oxygen consumption [27, 28]. In addition, abnormalities of tumor vascular bed may become the reason of venous blood outflow disorders [29]. High level of HHb in the aggressively growing tumor has been demonstrated earlier for rat model [30].

At the same time, abnormalities of tumor vascular bed may cause not only blood outflow disorders but also blood supply disorders which should be manifested by a simultaneous increase in the content of HHb and reduction of HbO_2 [29]. However, the absence of statistically significant changes in HbO_2 concentration observed in our study (figure 6) is an indicator of the stability of blood supply. Hence, there is no decrease in oxygen delivery rate which could potentially contribute to the tumor oxygenation reduction. It should be noted that combined effect of alteration in blood inflow, outflow and tissue oxygen consumption may results in insignificant total changes in HbO_2 content.

Revealed dependence between values of oxyhemoglobin concentration and tumor volume (figure 8(c)) allows

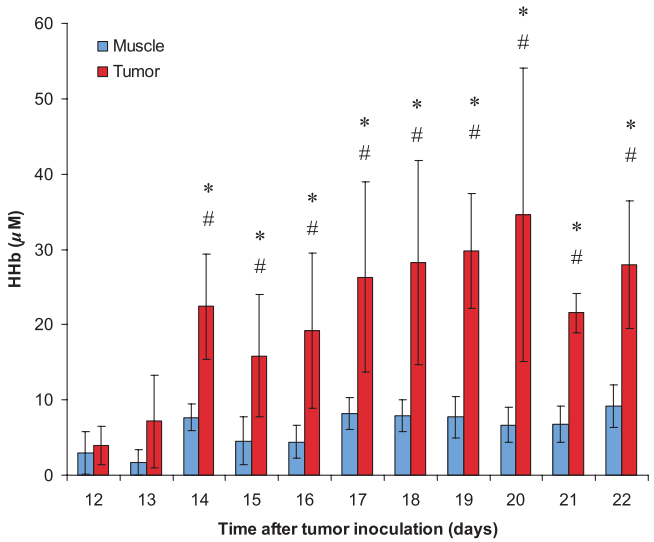

Figure 7. Dynamics of deoxyhemoglobin concentration in SKBR-3 tumor and in muscle. Asterisk (*) indicates statistically significant difference between the current and the initial values for tumor ($p < 0.05$). Hash (#) indicates statistically significant difference between current values for tumor and muscle ($p < 0.05$).

supposing even increase in HbO_2 contents in the course of tumor growth. To reveal the role of vessels structural changes in the processes of HbO_2 content increase additional morphological study is required. In addition, the ability to determine the blood flow rate simultaneously with oxy- and deoxyhemoglobin content [8] would make it possible to determine most accurately the reasons of SKBR-3 hypoxia formation.

Estimated values of tHb, HHb, HbO_2, and StO_2 correspond to the ranges obtained for animal tumors and normal tissues using DOS by other groups [14, 31]. The dynamics of tumor model oxygenation in the course of its growth is similar to that observed by authors of [32], who explained a gradual decrease

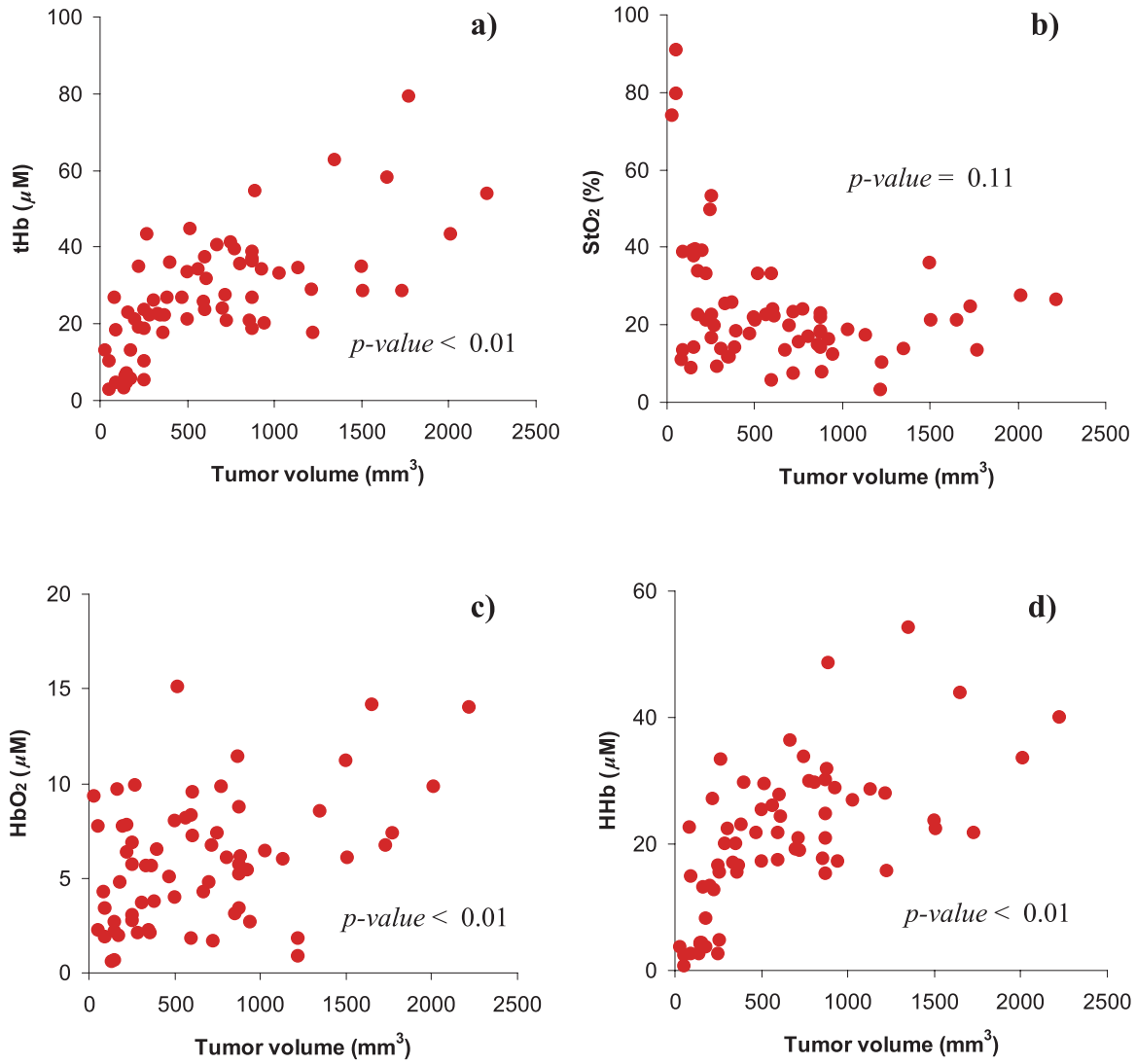

Figure 8. Values of tHb (a), StO_2 (b), HbO_2 (c), HHb (d) versus tumor volume for entire monitoring period for all mice (*p*-value is the significance level from χ^2-test).

of oxygenation of SCC VII model by the rise of oxygen consumption rate. In paper [14] the decrease of StO_2 level was observed in parallel with drop of oxyhemoglobin concentration and increase of deoxyhemoglobin content.

It is important to note that there is a systematic error in determination of hemoglobin concentration originated from the presence of myoglobin (Mb) in studied tissues having similar absorption spectra in the considered wavelength range [33]. According to [34], relative contribution of hemoglobin to the reconstructed absorption spectra obtained in mouse skeletal muscle is 80%. For variety of human tumors it was shown that Mb is synthesized at concentrations much lower than in striated muscle [35]. It has been demonstrated that breast tumor cells, including SKBR-3 cell line, also are capable to produce Mb [35, 36]. It should also be taken into account that Mb has a higher affinity for oxygen than Hb [37] that may affect the StO_2 level calculated from DOS measurements. In our study, we do not distinguish between myoglobin and hemoglobin, which may affect the results manifesting the increased level of hemoglobin and a higher level of oxygen saturation. We can suppose that the increased content of deoxy forms of both Hb and Mb may cause the decrease of oxygenation level in the course of tumor growth.

5. Conclusion

Using DOS technique, *in vivo* monitoring of oxygenation level and blood content in the course of experimental tumor growth was performed. Differences in the level of oxygenation and blood content between experimental tumor and normal tissue were revealed. It was demonstrated that rapid decrease of oxygenation level preceded the acceleration of its growth during which oxygen state has remained low. Increase of tumor volume was accompanied by the gradual increase of blood content, in which the main contribution was made by deoxyhemoglobin. We can conclude that the main reason of tumor oxygenation decrease is not the reduction of oxygen delivery to the tumor tissue rate, but, more likely, the increase of tissue oxygen consumption and decreased blood outflow rate. The proposed approach is useful for diagnosis of tumors as well as for study of changes in tumor models blood flow parameters when monitoring tumor response to therapy.

Acknowledgments

We wish to acknowledge the Targeted Federal Program of the Ministry of Education and Science of the Russian Federation, Grant No. 14.578.21.0030 (RFMEFI57814X0030). The authors are grateful to Prof Anna Maslennikova for fruitful discussions, to Kristina Kuznetsova for technical assistance in experiments, to Ilya Fiks for assistance in statistical analysis, and to Maksim Prudnikov and Vladimir Plekhanov for the engineering contribution to this work.

Disclosure

The authors have nothing to disclose.

References

[1] Quail D F and Joyce J A 2013 Microenvironmental *Nat. Med.* **19** 1423–37
[2] Finger E C and Giaccia A J 2010 *Cancer Metastasis Rev.* **29** 285–93
[3] Fan F, Schimming A, Jaeger D and Podar K 2012 *J. Oncol.* **2012** 281261
[4] Eriksen J E and Horsman M R 2006 *Radiother. Oncol.* **81** 119–21
[5] Jain R K 2013 *J. Clin. Oncol.* **31** 2205–19
[6] Vaupel P 2008 *Oncologist* **13** 21–6
[7] Durduran T, Choe R, Baker W B and Yodh A G 2010 *Rep. Prog. Phys.* **73** 076701
[8] Boas D A and Franceschini M A 2011 *Phil. Trans.* A **369** 4407–24
[9] McDonald D M and Choyke P L 2003 *Nat. Med.* **9** 713–25
[10] Ehling J, Lammers T and Kiessling F 2013 *Thromb. Haemost.* **109** 375–90
[11] Brown J Q, Wilke L G, Geradts J, Kennedy S A, Palmer G M and Ramanujam N 2009 *Cancer Res.* **69** 2919–26
[12] de Boer L L, Molenkamp B G, Bydlon T M, Hendriks B H, Wesseling J, Sterenborg H J and Ruers T J 2015 *Breast Cancer Res. Treat.* **152** 509–18
[13] Shaikh R, Prabitha V G, Dora T K, Chopra S, Maheshwari A, Deodhar K, Rekhi B, Sukumar N, Krishna C M and Subhash N 2016 *J. Biophoton.* at press (doi:10.1002/jbio.201500248)
[14] Vishwanath K, Yuan H, Barry W T, Dewhirst M W and Ramanujam N 2009 *Neoplasia* **11** 899–900
[15] Vishwanath K, Klein D, Chang K, Schroeder T, Dewhirst M W and Ramanujam N 2009 *J. Biomed. Opt.* **14** 054051
[16] Spliethoff J W, Evers D J, Jaspers J E, Hendriks B H, Rottenberg S and Ruers T J 2014 *Transl. Oncol.* **7** 230–9
[17] Rajaram N, Reesor A F, Mulvey C S, Frees A E and Ramanujam N 2015 *PLoS One* **10** e0117132
[18] Yu B, Lo J Y, Kuech T F, Palmer G M, Bender J E and Ramanujam N 2008 *J. Biomed. Opt.* **13** 060505
[19] Bender J E, Shang A B, Moretti E W, Yu B, Richards L M and Ramanujam N 2009 *Opt. Express* **17** 23396–409
[20] Shakhova N *et al* 2007 *Proc. SPIE* **6430** 64300N
[21] Calabro K, Curtis A, Galarneau J R, Krucker T and Bigio I J 2011 *J. Biomed. Opt.* **16** 011008
[22] Boswell C A *et al* 2014 *Mol. Pharm.* **11** 1591–8
[23] Loginova D A, Sergeeva E A, Krainov A D, Agrba P D and Kirillin M Yu 2016 *Quantum Electron.* **46** 528–33
[24] Oregon Medical Laser Center Website Optical properties spectra http://omlc.org/spectra/index.html (Accessed: 19 July 2016)
[25] Huang W, Ye M, Zhang L, Wu Q, Zhang M, Xu J and Zheng W 2014 *Mol. Cancer* **13** 150
[26] Safronova O and Morita I 2010 *J. Dent. Res.* **89** 430–44
[27] Honess D J, Kitamoto Y, Rampling M R and Bleehen N M 1996 *Br. J. Cancer* **74** S236–40
[28] Zywietz F, Böhm L, Sagowski C and Kehrl W 2004 *Strahlenther. Onkol.* **180** 306–14
[29] Fenton B M, Lord E M and Paoni S F 2001 *Int. J. Cancer* **93** 693–8
[30] Maslennikova A V *et al* 2010 *J. Biophoton.* **3** 743–51
[31] Pham T H, Hornung R, Berns M W, Tadir Y and Tromberg B J 2001 *Photochem. Photobiol.* **73** 669–77
[32] Fujii H, Sakata K, Katsumata Y, Sato R, Kinouchi M, Someya M, Masunaga S, Hareyama M, Swartz H M and Hirata H 2008 *Radiother. Oncol.* **86** 354–60
[33] Lorilee S L, Ciesielski W A, Thackray B D, Feigl E O and Schenkman K A 2010 *Appl. Spectrosc.* **64** 973–9
[34] Marcinek D J, Amara C E, Matz K, Conley K E and Schenkman K A 2007 *Appl. Spectrosc.* **61** 665–9
[35] Kristiansen G *et al* 2010 *Br. J. Cancer* **102** 1736–45
[36] Flonta S E, Arena S, Pisacane A, Michieli P and Bardelli A 2009 *Am. J. Pathol.* **175** 201–6
[37] Ordway G A and Garry D J 2004 *Exp. Biol.* **207** 3441–6